GEOPHYSICAL RESEARCH LETTERS, VOL. 36, L20609, doi:10.1029/2009GL040376, 2009

Assimilation of GRACE tide solutions into a numerical hydrodynamic inverse model

G. D. Egbert,[1] S. Y. Erofeeva,[1] S.-C. Han,[2,3] S. B. Luthcke,[2] and R. D. Ray[2]

Received 3 August 2009; revised 15 September 2009; accepted 30 September 2009; published 30 October 2009.

[1] We assimilate localized mass anomalies inferred from GRACE ranging measurements into a hydrodynamic model to improve tidal solutions around Antarctica for the M_2, S_2, and O_1 constituents. The variational approach used accounts for the spatial averaging of tidal elevations implicit in the mass anomaly parametrization used for the GRACE tidal analysis, as well as spatial correlation of errors in the resulting estimates. The inverse solution shows better agreement with independent station tide measurements around Antarctica, and it reduces cross-over residuals for ICESat laser altimeter data over the Filchner, Ronne and Ross Ice Shelves, demonstrating that GRACE data can provide useful constraints for improving hydrodynamic tidal models at high latitudes. **Citation:** Egbert, G. D., S. Y. Erofeeva, S.-C. Han, S. B. Luthcke, and R. D. Ray (2009), Assimilation of GRACE tide solutions into a numerical hydrodynamic inverse model, *Geophys. Res. Lett.*, *36*, L20609, doi:10.1029/2009GL040376.

1. Introduction

[2] The twin GRACE satellites [*Tapley et al.*, 2004], in orbit since March 2002, are sensitive detectors of mass changes at scales of a few hundred km and larger. This includes a large part of the the mass motions associated with oceanic tides [*Ray et al.*, 2003]. The gravity effects of tidal and other high-frequency motions must generally be removed from GRACE data to prevent aliasing into low-frequency (e.g., monthly) estimates of the gravity field. While ocean tide models are routinely used to accomplish this, the models are imperfect and residual tidal effects can be detected in both GRACE intersatellite ranging measurements [*Ray et al.*, 2009] and in GRACE gravity solutions [e.g., *Han et al.*, 2005; *Schrama et al.*, 2007; *Moore and King*, 2008]. Fortunately, with a sufficiently long time series of GRACE measurements available, such residual tide effects can be exploited to improve models.

[3] In a previous paper [*Han et al.*, 2007] we extracted residual tide solutions (i.e., solutions relative to an adopted prior model) around Antarctica for three major tidal constituents. The solutions were parametrized as localized average mass anomalies over areas approximately 300^2 km^2. The solutions appear to reveal useful new information about tides in a region not readily amenable to other kinds of measurements. Such long-wavelength tidal solutions are directly applicable to reprocessing GRACE data as well as to related kinds of orbit-determination calculations. They are not, however, of direct benefit to the multitude of other applications of ocean tide models which require higher spatial resolution. The present paper addresses that problem.

[4] In Section 2 we describe a scheme used for assimilating long-wavelength GRACE tide solutions into a numerical hydrodynamic model. This allows adjustment of a prior model at all wavelengths, in a rigorous way that satisfies the GRACE long-wavelength constraints as well as hydrodynamic constraints and other constraints from any other available kinds of data. We apply this technique to an update of our previous GRACE solutions [*Han et al.*, 2007]. In Section 4 we test the new adjusted solutions by using (a) semi-independent station tide measurements and (b) totally independent ICESat crossover data over the major Antarctic ice shelves.

2. Generalized Inversion of GRACE Solutions

[5] To assimilate GRACE tidal residuals we used the OSU Tidal Inversion Software (OTIS) [*Egbert and Erofeeva*, 2002], a relocatable system for variational data assimilation which estimates the tidal state $\mathbf{u}$ (elevations and currents) by minimizing, in a weighted least squares sense, misfits to the linear shallow water equations ($\delta\mathbf{f} = \mathbf{Su} - \mathbf{f}$) and to the observations ($\delta\mathbf{d} = \mathbf{d} - \mathbf{Lu}$). This is accomplished using the representer algorithm described by *Egbert and Erofeeva* [2002]. The scheme is based on the observation that the optimal solution takes the form

$$\hat{\mathbf{u}} = \mathbf{u}_0 + \sum_{k=1}^{K} b_k \mathbf{r}_k, \tag{1}$$

where $\mathbf{u}_0$ is the prior tidal solution, and $\mathbf{r}_k$ are the representers for the observation functionals L_k, $k = 1, \ldots K$. Once the representers (elevations and current fields) are computed by solving the forward and adjoint tidal equations (K times each), the vector of coefficients $\mathbf{b}$ in (1) can be obtained by solving the $K \times K$ system of equations

$$[\mathbf{R} + \mathbf{C_d}]\mathbf{b} = \mathbf{d} - \mathbf{Lu}_0, \tag{2}$$

where $R_{jk} = L_j \mathbf{r}_k$ and $\mathbf{C_d}$ is the data error covariance matrix.

[6] Assimilation of the GRACE data required only minor modifications to OTIS, primarily to allow for data functionals (L_k) corresponding to the elevation averages over rectangular domains, consistent with the parametrization of *Han et al.* [2007]. Because relatively few mass anomaly parameters were estimated in the GRACE tidal analysis (159 rectangular mass anomalies were fit for each constituent), K is small enough to allow computation of all

[1]College of Oceanic and Atmospheric Sciences, Oregon State University, Corvallis, Oregon, USA.
[2]NASA Goddard Space Flight Center, Greenbelt, Maryland, USA.
[3]GEST, University of Maryland, Baltimore County, Baltimore, Maryland, USA.

0094-8276/09/2009GL040376$05.00

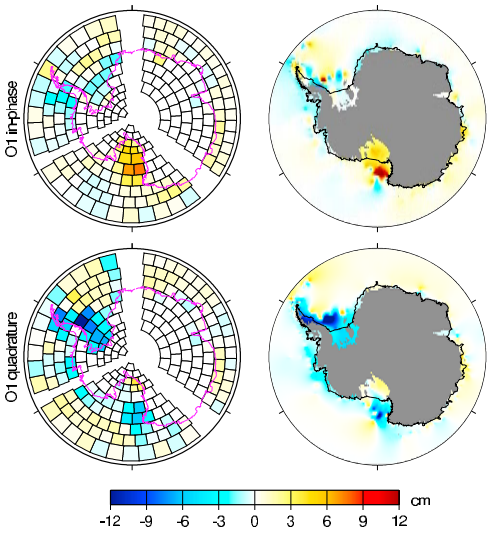

Figure 1. The O_1 tidal constituent, relative to our prior model, (left) before and (right) after assimilation—i.e., the Figure 1 (left) shows our initial GRACE solution; Figure 1 (right) shows the final assimilated adjustments that we then add to our prior tide model. (top) Diagrams are in-phase components; (bottom) quadrature components. In a few locations the solutions saturate our color scale; the largest amplitude in the assimilation solution reaches 21 cm in the Weddell Sea.

representers. It is then straightforward to directly form and solve (2), allowing use of the full data error covariance, which can be obtained from propagation of errors in the analysis of *Han et al.* [2007]. We applied this scheme to derive large-scale corrections in the vicinity of Antarctica for TPXO.7.1, a $^1/_4°$, fully global inverse tidal model constrained primarily by TOPEX/Poseidon and Jason altimetry data. Bathymetry data for TPXO.7.1, and for the GRACE assimilation, were taken from a combination of *Smith and Sandwell* [1997] and, south of 56°S, *Padman et al.* [2002]. The model error covariance, based on the formulation of *Egbert and Erofeeva* [2002] was tapered to zero north of 55°S, to keep corrections to the global model small outside the area covered by the GRACE tidal solutions of *Han et al.* [2007].

[7] For the present study we have updated the GRACE residual tidal mass-anomaly estimates primarily by improved removal of non-tidal signals in the intersatellite range-rate data, and by incorporation of another 12 months of range-rate data, for a total timespan of approximately four years (April 2003 to April 2007). For removal of variable atmospheric mass effects we used 3-hourly operational weather analysis outputs from the European Centre for Medium-range Weather Forecasting (ECMWF); for non-tidal ocean mass variations we used 6-hourly outputs from the Toulose Unstructured Grid Ocean Model, run in barotropic mode and forced by 6-hourly ECMWF pressures and winds [*Carrère and Lyard*, 2003]; for land hydrology mass variations we used outputs from the Global Land Data Assimilations System [*Rodell et al.*, 2004]; and finally for mantle glacial rebound we used the ICE-5G (VM2) model of *Peltier* [2004]. Model TPXO7.1, which we used as the prior for our data assimilation, was also used as the tide model for our GRACE processing.

[8] Of the four major tidal constituents we solved, as before, for the principal lunar diurnal wave O_1 and the principal lunar and solar semidiurnal waves M_2 and S_2, respectively. The diurnal declinational wave K_1, however, is still too unstable to estimate reliably from GRACE owing to its long alias period of 7.5 years [*Ray et al.*, 2003].

3. Results

[9] Figure 1 shows results for the O_1 tidal constituent before and after the assimilation process. The mean mass anomalies resulting from our initial GRACE inversions (left column) are seen to be, as expected, a somewhat blurred representation of the final O_1 solutions (right column). (Note that both before and after diagrams are relative to our prior model.) The largest resulting O_1 amplitude adjustments are in the Weddell Sea, reaching 21 cm near 72°S, 54°W, and in the Ross Sea, reaching 18 cm near 74°S, 177°E. The latter location corresponds to the shallow Pennell Bank, where the bathymetry rises to about 400 m.

[10] In both the Weddell and Ross Seas the hydrodynamic elevation corrections exhibit an alternating pattern of short-wavelength highs and lows, suggestive of shelf waves propagating along the continental slope, as can be confirmed by examination of the corresponding current corrections (not shown). This underlines the critical role that assimilation plays in developing improved models with satellite gravity data. The large-scale mass anomalies (in Figure 1, left) are of little benefit to any application other than satellite orbit determination or GRACE data reprocessing. Assimilation assures a hydrodynamically consistent final product, with scales appropriate to the true tidal waves.

[11] Figure 2 shows results for the M_2 constituent. There is hardly any adjustment in the Ross Sea region, but this reflects the unusually small amplitudes of M_2 there—an amphidrome in fact sits near the center of the ice shelf [*MacAyeal*, 1984]. In contrast, M_2 amplitudes are relatively large in the Weddell Sea region, and both pre- and post-

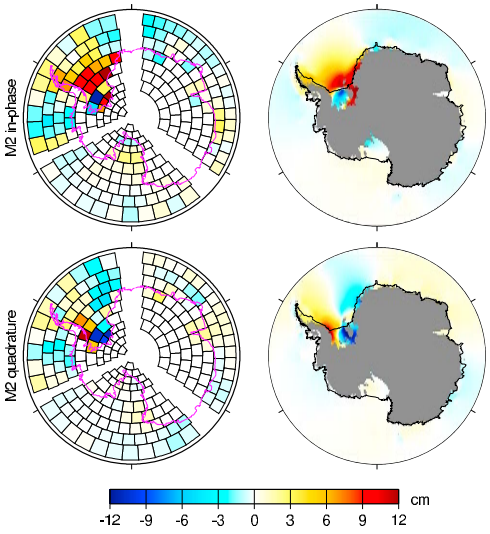

Figure 2. As in Figure 1, except for the M_2 constituent. As before, a few locations saturate the color scale.

Table 1. Tide Gauge RMS Differences (cm)[a]

	M_2			S_2			O_1		
Constituent Tide Model	FES	TPXO	GRACE	FES	TPXO	GRACE	FES	TPXO	GRACE
ALL	4.01	3.74	3.02	4.57	3.14	2.96	5.26	5.35	4.03
NA	4.17	4.45	3.45	5.15	4.22	3.93	5.81	6.20	5.20
Assim	3.88	3.06	2.63	4.05	1.88	1.86	4.78	1.85	2.77
Rsea	4.93	3.08	2.89	2.45	3.08	3.08	6.02	3.22	3.65
Wsea	3.86	4.41	3.37	6.00	3.01	2.73	5.68	5.45	4.77
Other	2.42	2.59	2.18	2.03	3.51	3.29	1.08	1.93	2.05

[a]FES: FES2004. TPXO, TPXO7.1. ALL: based on all 61 tide stations. NA: based on station data not assimilated in either model. Assim: based on station data assimilated in TPXO.7.1. Rsea, Wsea: based on stations on the Ross and Weddell ice, respectively. Other: based on stations elsewhere.

assimilation diagrams show correspondingly large adjustments to our prior model. The largest adjustments—approximately 20 cm—are along the southern boundary of the Weddell, under the Filchner Ice Shelf south of Berkner Island.

4. Comparisons Against Independent Data

[12] To evaluate these solutions it is essential to compare with independent measurements. Aside from a few well-maintained tide gauges (e.g., Faraday Base) independent measurements in this region tend to be sparse, gappy, and of short duration and are therefore somewhat problematic for testing purposes. Much of our available data are located on the major ice shelves, where tidal elevations have been extracted from gravimeter or GPS stations. The largest ice shelves appear to float freely on the underlying ocean tide except within a few km of the grounding zone [*Fricker and Padman*, 2006].

4.1. Station Tide Measurements

[13] As a first test we use the compilation of Antarctic harmonic constants of *King and Padman* [2005] to test three tide models: our prior TPXO7.1, our assimilation solution, and FES2004 [*Lyard et al.*, 2006], which was selected because of its widespread adoption by the geodetic community. For this comparison we used only tide gauges with at least 29 days of data which are located within the $^1/_4°$ TPXO7.1 ocean grid and are poleward of 59.5°S. Of the 61 such gauges, 34 had been assimilated already in the global solution used for the prior, and 27 had not; 31 gauges were located in the Weddell Sea and 18 in the Ross Sea, with the remaining 12 distributed around the rest of Antarctica. Vector root mean square (RMS) differences were computed for the full tide gauge set, for the non-assimilated and assimilated gauges, and for each of the geographic subgroups. Results are shown in Table 1. The GRACE assimilation solution is in best agreement with harmonic constants for all three constituents, whether all, or only the unassimilated, set of gauges are considered. There are even small reductions in RMS for the group of previously assimilated gauges for the two semi-diurnal constituents. Results for individual geographic areas are more variable, though the GRACE assimilation solution generally improves on both of the global solutions, sometimes significantly.

4.2. ICESat Laser Altimetry

[14] As a second test of our inversions we use ICESat laser altimeter data over the major Antarctic ice shelves. The RMS of crossover differences for this satellite (computed from elevation differences at intersections of ascending and descending arcs) has been shown to be sensitive to the model used to remove tidal variations from the altimetry [*Padman and Fricker*, 2005].

[15] A set of laser altimeter crossover differences were formed from the first fourteen ICESat operational periods, each roughly 30 days in duration. Only intra-period crossovers are used here, although inter-period data could be somewhat more sensitive to the S_2 tide because of its long alias [*Ray*, 2008]. Data were corrected for detector saturation and were also adjusted for atmospheric loading based on an inverted barometer response (which was found to reduce crossover discrepancies). Outlier detection was based on several tests, before and after binning by geographic location, but as seen below this task was only partially successful. We use these crossovers to test the same three models compared against the tide gauges. Data are restricted to two zones: the Filchner and Ronne Ice Shelves (FRIS) and the Ross Ice Shelf (RIS). Other ice shelves of potential interest such as the Larsen and Amery have too few data for reliable statistics. For the FRIS and RIS we have 11,181 and 31,952

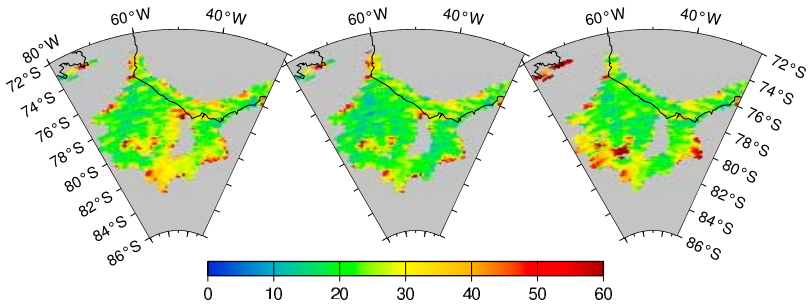

Figure 3. Mean ICESat crossover discrepancies (cm) over the Filchner and Ronne Ice Shelves as function of adopted tide model: (left) TPXO7.1, (middle) this paper, (right) FES2004. Corresponding RMS statistics for this region are tabulated in Table 2.

Table 2. ICESat RMS Crossover Differences (cm) Obtained With No Tidal Correction and With the Three Solutions Discussed in the Text

Tide Model	FRIS	RIS
None	133.4	70.8
FES2004	37.4	43.6
TPXO7.1	36.1	31.5
This paper	31.2	31.4

crossovers, respectively; the latter is greater because it is closer to the pole where altimeter intersections are very dense.

[16] Figure 3 shows mean crossover differences, mapped in overlapping 3° (longitude) × 0.5° (latitude) bins, for the FRIS region of the southern Weddell Sea. The charts are somewhat noisy, with small red patches suggesting ICESat outliers. However, closer examination of some of these patches suggests that tide model error is also a contributing cause; for example, just north of the Henry Ice Rise (80°S, 65°W) a preliminary tidal analysis of the ICESat altimetry suggests that both TPXO7 and FES2004 are in error by tens of cm. Aside from these localized patches, it is clear that our assimilated tidal solution results in improved crossover differences. Especially noticeable is the zone of reduced differences along the western and southern sides of Berkner Island, extending southwards all the way to the Ronne grounding zone. The FES2004 chart appears already superior to TPXO7 in part of that region, but it shows much larger tide errors along the entire southwest boundary of the ice shelf.

[17] A similar figure for the Ross Ice Shelf shows far less improvement from our assimilation, probably because the smallness of all semidiurnal tides implies that only our adjustment of O_1 is being tested. As Figure 1 shows, the O_1 adjustments over the RIS are fairly small—less than 5 cm in the in-phase component. Unfortunately, we have no test data for the much larger adjustments near Pennell Bank in the open Ross Sea.

[18] RMS crossover differences for both ice-shelf regions are tabulated in Table 2. In keeping with Figure 3 the statistics indicate good improvement over the FRIS region from our GRACE assimilation, but less over the RIS. The relatively poorer performance of FES2004 over the RIS arises almost entirely from evident errors in their adopted ice shelf grounding line [see also *Ray*, 2008, Figure 4].

5. Conclusions

[19] Assimilation of the GRACE data into a tidal model was accomplished in two rather complex, but only loosely coupled stages: the range rate data were first fit to a spatially coarse model of periodic mass variations, and then the results were fit to a much higher resolution tidal model, constrained by the hydrodynamic equations. By using the full error covariance from the first stage to define the misfit norm for the assimilation, coupling between the two stages is improved—only the well resolved part of the mass anomaly parameter space is fit in the second stage.

[20] The shelf waves that can be clearly seen in the hydrodynamic correction for O_1 (Figure 1) have short spatial scales, which are already not well resolved by the parametrization of mass anomalies, or indeed by the GRACE data. Rather, such small-scale features result from the hydrodynamic equations, which the assimilation solution must satisfy (albeit approximately) while simultaneously reproducing the gravitational signal observed by GRACE. Fine scale details which are not directly constrained by the data, such as the exact phase of the shelf waves, may still be poorly determined and should probably be interpreted with some caution.

[21] However, comparisons with independent data clearly demonstrate that the GRACE data can now be used to constrain and improve hydrodynamic tidal models, at least at large scales, and for major constituents that are temporally resolved by the GRACE orbit. As the length of the mission increases further improvements can be expected—e.g., it should soon be possible to obtain, and assimilate, stable solutions for K_1, as well as smaller constituents such as N_2, K_2 and P_1. This additional source of tidal data will be particularly valuable at high latitudes where high quality altimetry data are lacking.

[22] **Acknowledgments.** We thank D. Rowlands and J.-P. Boy for help with processing of GRACE data. This work was supported by the National Aeronautics and Space Administration's GRACE and International Polar Year projects.

References

Carrère, L., and F. Lyard (2003), Modeling the barotropic response of the global ocean to atmospheric wind and pressure forcing: Comparisons with observations, *Geophys. Res. Lett.*, *30*(6), 1275, doi:10.1029/2002GL016473.

Egbert, G. D., and S. Y. Erofeeva (2002), Efficient inverse modeling of barotropic ocean tides, *J. Atmos. Oceanic Technol.*, *19*, 183–204.

Fricker, H. A., and L. Padman (2006), Ice shelf grounding zone structure from ICESat laser altimetry, *Geophys. Res. Lett.*, *33*, L15502, doi:10.1029/2006GL026907.

Han, S.-C., C. K. Shum, and K. Matsumoto (2005), GRACE observations of M_2 and S_2 ocean tides underneath the Filchner-Ronne and Larsen ice shelves, Antarctica, *Geophys. Res. Lett.*, *32*, L20311, doi:10.1029/2005GL024296.

Han, S.-C., R. D. Ray, and S. B. Luthcke (2007), Ocean tidal solutions in Antarctica from GRACE inter-satellite tracking data, *Geophys. Res. Lett.*, *34*, L21607, doi:10.1029/2007GL031540.

King, M. A., and L. Padman (2005), Accuracy assessment of ocean tide models around Antarctica, *Geophys. Res. Lett.*, *32*, L23608, doi:10.1029/2005GL023901.

Lyard, F., F. Lefèvre, T. Letellier, and O. Francis (2006), Modeling the global ocean tides: Insights from FES2004, *Ocean Dyn.*, *56*, 394–415.

MacAyeal, D. R. (1984), Numerical simulations of the Ross Sea tides, *J. Geophys. Res.*, *89*, 607–615.

Moore, P., and M. A. King (2008), Antarctic ice mass balance estimates from GRACE: Tidal aliasing effects, *J. Geophys. Res.*, *113*, F02005, doi:10.1029/2007JF000871.

Padman, L., and H. A. Fricker (2005), Tides on the Ross Ice Shelf observed with ICESat, *Geophys. Res. Lett.*, *32*, L14503, doi:10.1029/2005GL023214.

Padman, L., H. A. Fricker, R. Coleman, S. Howard, and S. Erofeeva (2002), A new tidal model for the Antarctic Ice shelves and seas, *Ann. Glaciol.*, *34*, 247–253.

Peltier, W. R. (2004), Global glacial isostatic adjustment and the surface of the ice-age earth: The ICE-5G model and GRACE, *Annu. Rev. Earth Planet. Sci.*, *32*, 111–149.

Ray, R. D. (2008), A preliminary tidal analysis of ICESat laser altimetry: Southern Ross Ice Shelf, *Geophys. Res. Lett.*, *35*, L02505, doi:10.1029/2007GL032125.

Ray, R. D., D. D. Rowlands, and G. D. Egbert (2003), Tidal models in a new era of satellite gravimetry, *Space Sci. Rev.*, *108*, 271–282.

Ray, R. D., S. B. Luthcke, and J.-P. Boy (2009), Qualitative comparisons of global ocean tide models by analysis of intersatellite ranging data, *J. Geophys. Res.*, *114*, C09017, doi:10.1029/2009JC005362.

Rodell, M., et al. (2004), The global land data assimilation system, *Bull. Am. Meteorol. Soc.*, *85*, 381–394.

Schrama, E. J. O., B. Wouters, and D. A. Lavallée (2007), Signal and noise in Gravity Recovery and Climate Experiment (GRACE) observed surface mass variations, *J. Geophys. Res.*, *112*, B08407, doi:10.1029/2006JB004882.

Smith, W. H. F., and D. T. Sandwell (1997), Global seafloor topography from satellite altimetry and ship depth soundings, *Science*, *277*, 1957–1962.

Tapley, B. D., S. Bettadpur, J. Ries, P. Thompson, and M. Watkins (2004), GRACE measurements of mass variability in the Earth system, *Science*, *305*, 503–505.

G. D. Egbert and S. Y. Erofeeva, College of Oceanic and Atmospheric Sciences, 104 COAS Admin Bldg., Corvallis, OR 97331-5503, USA. (egbert@coas.oregonstate.edu)

S.-C. Han, S. B. Luthcke, and R. D. Ray, NASA Goddard Space Flight Center, Code 698, Greenbelt, MD 20771, USA. (richard.ray@nasa.gov)